Identification and detection of gaseous effluents from hyperspectral imagery using invariant algorithms

Erin M. O'Donnell, David W. Messinger, Carl Salvaggio, and John R. Schott

Digital Imaging and Remote Sensing Laboratory
Chester F. Carlson Center for Imaging Science
Rochester Institute of Technology, 54 Lomb Memorial Drive, Rochester, NY

ABSTRACT

The ability to detect and identify effluent gases is, and will continue to be, of great importance. This would not only aid in the regulation of pollutants but also in treaty enforcement and monitoring the production of weapons. Considering these applications, finding a way to remotely investigate a gaseous emission is highly desirable. This research utilizes hyperspectral imagery in the infrared region of the electromagnetic spectrum to evaluate an invariant method of detecting and identifying gases within a scene. The image is evaluated on a pixel-by-pixel basis and is studied at the subpixel level. A library of target gas spectra is generated using a simple slab radiance model. This results in a more robust description of gas spectra which are representative of real-world observations. This library is the subspace utilized by the detection and identification algorithms. The subspace will be evaluated for the set of basis vectors that best span the subspace. The Lee algorithm will be used to determine the set of basis vectors, which implements the Maximum Distance Method (MaxD). A Generalized Likelihood Ratio Test (GLRT) determines whether or not the pixel contains the target. The target can be either a single species or a combination of gases. Synthetically generated scenes will be used for this research. This work evaluates whether the Lee invariant algorithm will be effective in the gas detection and identification problem.

Keywords: gaseous effluents, invariant algorithms, hyperspectral imagery, plumes, target detection

1. INTRODUCTION

Determining the composition of a plume is important for the environmental community both domestically and abroad. This would aid in the regulation of pollutants by the environmental monitoring organizations as well as assist treaty enforcement and the monitoring of weapons productions. Algorithm utility for this gas problem involves detecting and locating the gas cloud, identifying the gas species, quantifying the mixing ratio, and ultimately concentration prediction. The focus of this research is the detection and identification aspect of the algorithm development process. This work evaluated the Lee algorithm[1,2] for this gas detection and identification problem within a hyperspectral scene.

The Lee algorithm was developed to disregard variations in a target due to atmospheric and illumination conditions and is inherently a sub-pixel detection algorithm. This implementation utilizes the invariant nature of the algorithm to overcome temperature and concentration variations within a gas cloud. The Lee algorithm utilizes the Maximum Distance Method (MaxD)[1] to select target basis vectors.

There are many issues that make this work difficult. The targets in this case are transparent gases and can be seen in emission or absorption, often within the same plume. The background has to be taken into account when looking at these features. Multiple gas releases can have spectrally overlapping features that make separability difficult. Atmospheric gases can also potentially mask gas features or confuse algorithms as to whether it is a plume gas or an atmospheric constituent.

Further author information: (Send correspondence to E. O'Donnell)
E. O'Donnell: E-mail: emo1683@rit.edu, Telephone: 1 585 475 4503

Algorithms and Technologies for Multispectral, Hyperspectral, and Ultraspectral Imagery X, edited by Sylvia S. Shen, Paul E. Lewis, Proceedings of SPIE Vol. 5425 (SPIE, Bellingham, WA, 2004) · 0277-786X/04/$15 · doi: 10.1117/12.542426

Lisowski and Cook (1996)[3] assessed the use of shortwave and midwave infrared (MWIR) hyperspectral imagery to identify SO_2 emitted from a coal burning power plant. Their study evaluated three algorithms for determining if this chemical was present. One algorithm that was used, which was most influential to this work was Singular Value Decomposition (SVD). The results of the study showed that SVD can be used to determine the extent of the chemical plume from ground collected imagery.

Thai and Healey (2002)[4] developed a sub-pixel invariant algorithm for material detection in the visible (VIS) and near infrared (NIR) of a specific target spectrum under any illumination or atmospheric conditions. This algorithm implements SVD and then a maximum likelihood classification. This algorithm when compared to the widely used Spectral Angle Mapper (SAM) provided less false detections.

Young (2002)[5] reviewed processes for gas detection and quantification using Spatially Enhanced Broadband Array Spectrograph System (SEBASS) imagery. One of the processes reviewed for gas detection was SVD, which was able to find significant plumes in imagery that had yet to be atmospherically corrected. Although Young did a robust study there was still room for further research. Young had *a priori* knowledge of the gases in the scene. The work described in the paper assumes nothing about the scene, not even the presence of a plume. Young mentioned that most of the gases in his study have spectral absorption coefficients that do not vary with temperature over the temperature range of interest (15 – 80^{o}C). This work, in contrast, utilizes spectra measured at multiple temperatures for the target gases. Also, the target space considers both emission and absorption features.

This document is organized in the following way. First, it describes the Lee algorithm and in what way it supports this research. Second is a discussion of the how the target space is generated along with the supporting radiance model. The test data and imagery is then introduced along with a discussion of the synthetic image generator, DIRSIG.[6] Finally, results of the application of this algorithm are presented with future directions for this research.

2. INVARIANT METHOD

Lee (2003)[1] developed an invariant algorithm that addressed sub-pixel material identification under varying illumination and atmospheric conditions, similar to Thai and Healey's algorithm.[4] This implementation utilizes a new method of generating target and background basis vectors, incorporating the Maximum Distance Method (MaxD) technique that results in linearly independent basis vectors. By viewing the target subspace in an n-dimensional form, the corners of the simplex enclosing the target vectors are the points that are the maximum distance from any point within the simplex. These points are found by first determining the vector at the most extreme point from the origin and that closest to the origin. These points are now considered corners of the simplex. The difference vector is found between these two points and a plane perpendicular to the difference vector is determined. The data points are then projected onto this plane and the new point furthest from the first vector is found as the next end-member. This process is repeated until all the data points are collapsed onto one point. Linear combinations of those basis vectors will recreate all the data contained within the simplex. Then the basis vectors are compared to the image using the Generalized Likelihood Ratio Test (GLRT). For consistency the notation here will be the same at that used in Bajorksi, *et al.* (2004).[7] A image pixel can be described as

$$\mathbf{x} = \mathbf{Ta} + \mathbf{Bb} + \epsilon \tag{1}$$

where $\mathbf{x}$ is the pixel, $\mathbf{T}$ and $\mathbf{B}$ respectively are the target and background basis vector matrices, and $\mathbf{a}$ and $\mathbf{b}$ are the abundance vectors of each material. The error in the modeling process and or the data is taken into account in the vector ϵ. The hypothesis test is then

$$H_0 : \mathbf{a} = \mathbf{0} \tag{2}$$

for the target absent from the pixel and

$$H_1 : \mathbf{a} \neq \mathbf{0} \tag{3}$$

for the opposite situation. Then the GLRT can be written as

$$GLR(\mathbf{x}) = [MSD(\mathbf{x}) + 1]^{p/2}, \tag{4}$$

where the MSD operator is the matched subspace detector and p is the number of bands. The matched subspace detector is futher described as

$$MSD(\mathbf{x}) = \frac{\mathbf{x^T}(\mathbf{P_B^\perp} - \mathbf{P_Z^\perp})\mathbf{x}}{\mathbf{x^T}\mathbf{P_Z^\perp}}. \tag{5}$$

Here $\mathbf{Z}$ is a matrix composed of all target and basis vectors, and $\mathbf{P_Y^\perp}$ is the martix created by projecting all the columns $\mathbf{Y}$ onto a space orthogonal to it, where $\mathbf{B}$ or $\mathbf{Z}$ can be substituted for $\mathbf{Y}$. For a more thorough explanation of this algorithm and the MSD operator the reader is referred to Bajorski, *et al.* (2004).[7]

3. TARGET SPACE GENERATION

The gases that this study attempts to detect are from the list of the top hazardous gases according to the the United States Environmental Protection Agency's Clean Air Act (www.epa.gov/airtrends/toxic2.html). These gas absorption spectra were obtained from the Pacific Northwest National Laboratory (PNNL) (Sharpe, *et al.*, 2001)[8] (nwir.pnl.gov). For each of these gas signatures, a subspace was generated describing various temperatures and concentrations of the gas. The subspace for this work was populated with target radiance vectors generated in the following way.

The target space was described by a radiance model as shown in Equation 6

$$L(\lambda) = [\epsilon_s(\lambda)B(\lambda, T_s)\tau_p(\lambda) + \epsilon_p(\lambda)B(\lambda, T_p)]\tau_a(\lambda) + L_u(\lambda) + L_n(\lambda), \tag{6}$$

where $L(\lambda)$ is the total radiance. This is expressed in terms of the Planckian radiance, $B(\lambda, T_s)$, at the temperature of the surface, T_s attenuated by the emissivity of the surface, $\epsilon_s(\lambda)$, and the transmission of the plume, $\tau_p(\lambda)$, which is added to the Planckian radiance, $B(\lambda, T_p)$, at the plume temperature, T_p, attenuated by the emissivity of the plume, $\epsilon_p(\lambda)$; this is then all multiplied by the transmission of the atmosphere, $\tau_a(\lambda)$, and finally, the upwelled radiance, $L_u(\lambda)$, and the noise radiance, $L_n(\lambda)$, are added to that. This representation will be referred to as the single slab model. In this discussion the term slab refers to a homogenous mass that has a consistent temperature and concentration throughout.

Using Kirkoff's Law and assuming the plume is optically thin the transmission of the plume, $\tau_p(\lambda)$, can further be described as

$$\tau_p(\lambda) = 1 - \epsilon_p(\lambda), \tag{7}$$

$$\epsilon_p(\lambda) = 1 - ck(\lambda, T_g), \tag{8}$$

where c is the concentration path length of the gas, and $k(\lambda, T)$ is the absorption spectrum of the gas at a particular temperature from the PNNL database. Equation 8 assumes the plume is optically thin. Each gas within the PNNL database is measured at three different temperatures, T_g, (5^oC, 25^oC, 50^oC). The target subspace is generated with plume gas spectra at concentration and temperature ranges between 1-1000 ppm-m and 5-30^oC, respectively. The subspace then contains 64 vectors for each gas, some of which are shown in Figures 2 and 3. Basis vectors are selected from this library using MaxD.

In this study $\tau_a(\lambda)$ and the $L_u(\lambda)$ terms were generated by running a MODTRAN mid-latitude summer atmosphere and are held constant between runs. More specifically, there is no atmospheric variability in the target space. Also, the system noise, $L_n(\lambda)$, is assumed to be negligible. The downwelled term is disregarded because of the assumed high emissivity of the background which results in low reflective value. Furthermore, the reflected downwelled term will be even less significant and is therefore also ignored.

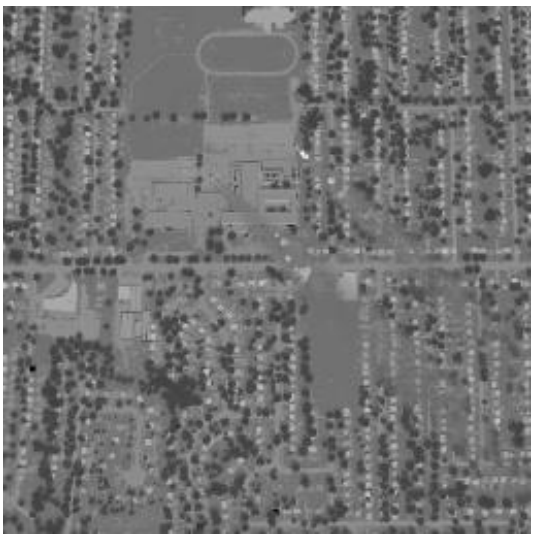

Figure 1. The test DIRSIG scene[9] prior to processing at $10.73\mu m$. Within the scene are two faint plumes extending from the upper center to the lower right.

4. TEST DATA SET

The test scene was generated using a synthetic image generator, DIRSIG.[6] This simulation environment allows physics-based hyperspectral scenes to be generated with truth maps. Some examples of the truth maps are the temperature of each pixel in the image (plume, background, etc.) as well as concentration of the gas species. The material spectra used in these scenes were measured in either the field or the laboratory. This scene has varying backgrounds of trees, buildings, grass, parking lots, etc. This allows for simple and complex plume pixel scenarios, as shown in Figure 1. The sensor model that is incorporated into these simulated scenes is similar to that of the SEBASS instrument. The difference is that the simulation does not, in this scene incorporate, the sensor noise. Also, the simulated scene is only using the longwave infrared (LWIR), whereas the actual sensor images in both the MWIR and LWIR. The plumes are generated within DIRSIG using the Jet Propulsion Lab (JPL) plume model.[10] This model implements a Gaussian concentration and temperature distribution orthogonal to the downwind direction and exponential distribution downwind. The JPL model is considered to be spectrally accurate although spatially it is lacking. For more information on DIRSIG and the plume model refer to Schott, *et al.* (1999)[6] and Kuo (2000)[11] respectively. The plumes in this test scene each consist of a single gas release. The upper plume contains freon (Fr-114) and the lower plume contains ammonia (NH_3). The basis vectors from MaxD describing these gases are shown in Figures 2 and 3.

For the Lee algorithm a background subspace is also necessary. A DIRSIG scene was generated without the plumes included. Then MaxD was run on this to obtain the background basis vectors, some of which are shown in Figure 4. Ultimately if using real data, a region of interest within the scene in an area where there was assumed to be no plume would be an appropriate input to MaxD to find the background basis vectors.

5. RESULTS

The output of the GLRT is a hyperspectral image of likelihood maps where the bands represent the target gases as described in Table 1. A pixel from the GLRT image located in the freon plume is shown in Figure 5. By referencing Table 1, the band with the highest value in this spectrum corresponds to that of freon. The GLRT image of the freon band (Figure 6) distinctly shows the plume. A pixel investigated in the ammonia plume (Figure 7) returns a high value in band 20, which corresponds to ammonia. The ammonia plume, in band 20 (Figure 8) shows up less distinctly and with more returns from the background. This is not too concerning, however, as ammonia is an atmospheric gas and is possibly reflected off low emissivity background materials in

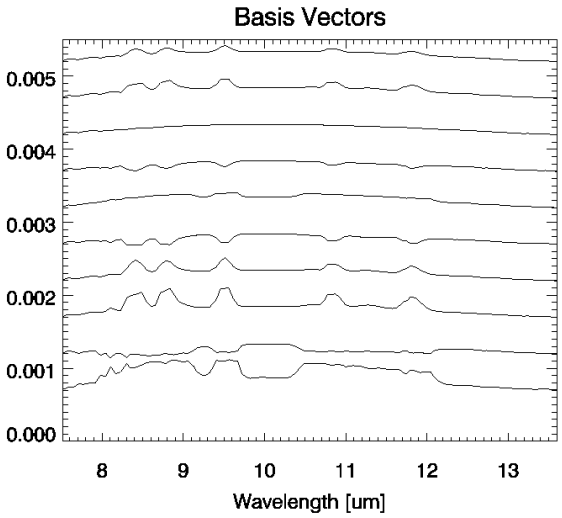

Figure 2. Target basis vector set resulting from application of the MaxD algorithm to the freon target space (plots are offset for clarity).

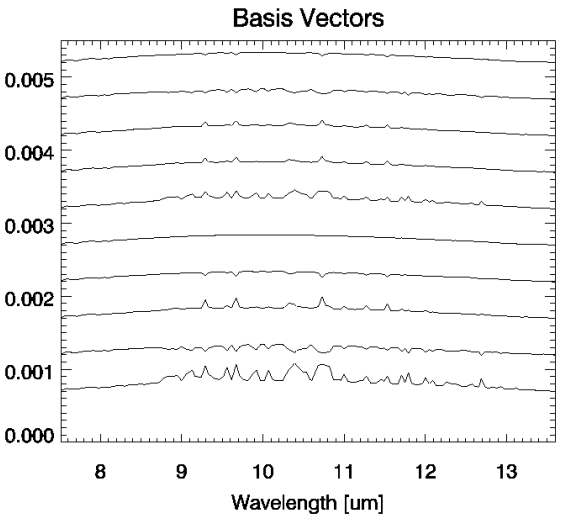

Figure 3. Target basis vector set resulting from application of the MaxD algorithm to the NH_3 target space (plots are offset for clarity).

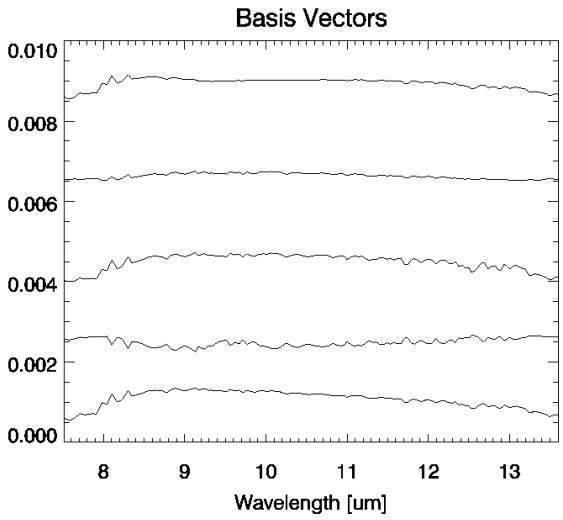

Figure 4. Some of the background basis vectors (plots are offset for clarity).

Table 1. Band numbers as they correspond to gases

Band Index	Gas	Band Index	Gas
0	Acrolien	14	Freon-125
1	Fluorobenzene	15	Freon-12
2	Benzene	16	Freon-134a
3	Carbon tetrachloride	17	Freon-218
4	Methyl chloride	18	Formaldehyde
5	Methane	19	Hydrogen chloride
6	Carbon dioxide	20	Ammonia
7	Carbon monoxide	21	Phosgene
8	Dichloromethane	22	Sulfur hexafloride
9	1,2-Dichloropropane	23	Sulfur dioxide
10	1,3-Dichloropropane	24	1,1,2,2-Tetrachloroethane
11	1,2-Dibromomethane	25	Tetrachloroethane
12	1,2-Dichloromethane	26	Vinyl chloride
13	Freon-114		

these areas. Another evaluation is made by comparing the plume pixel regions to a background pixel (Figure 9). Here the magnitude of the return in the plume bands of the corresponding plume gases is significantly higher than any of the returns in any of the gas bands in the background pixel.

6. CONCLUSION AND FUTURE WORK

Initial results point toward the Lee Algorithm as a significant resource for the gas detection and identification problem. The algorithm succeeds with both non-atmospheric native gases and atmospheric native gases. Also, it is capable of handling both the emission and absorption areas within the plumes. A more robust target space

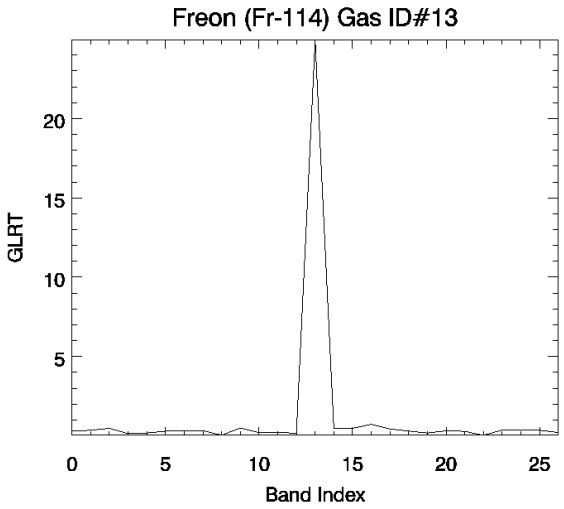

Figure 5. GLRT results for a pixel in the freon plume for all gases in the target set. Freon is gas no. 13.

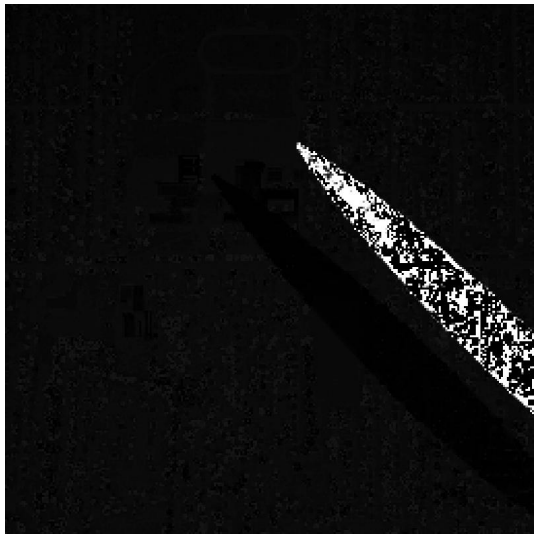

Figure 6. Detection map resulting from application of the freon target space to the image.

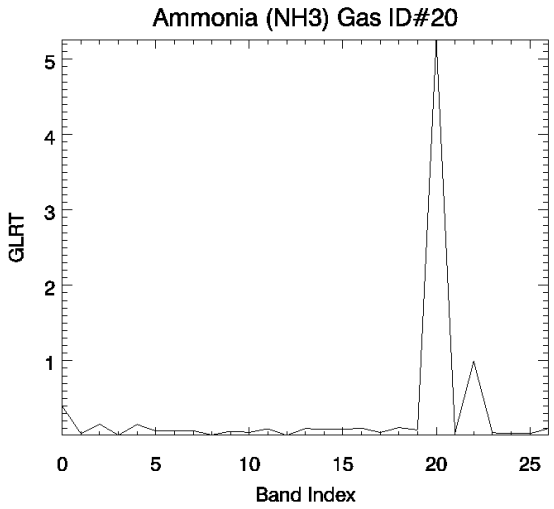

Figure 7. GLRT results for a pixel in the NH_3 plume for all gases in the target set. NH_3 is gas no. 20.

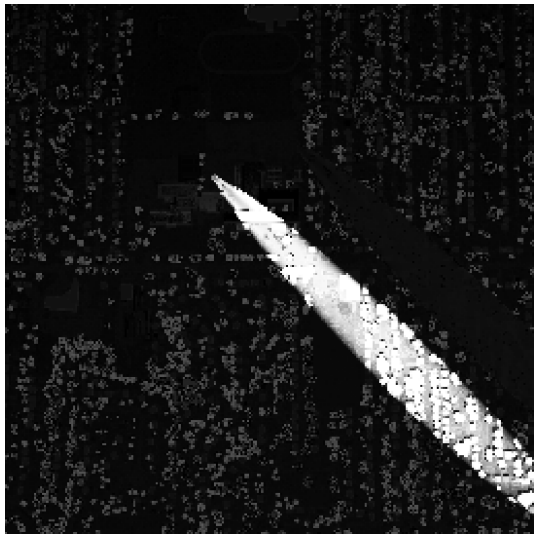

Figure 8. Detection map resulting from application of the NH_3 target space to the image.

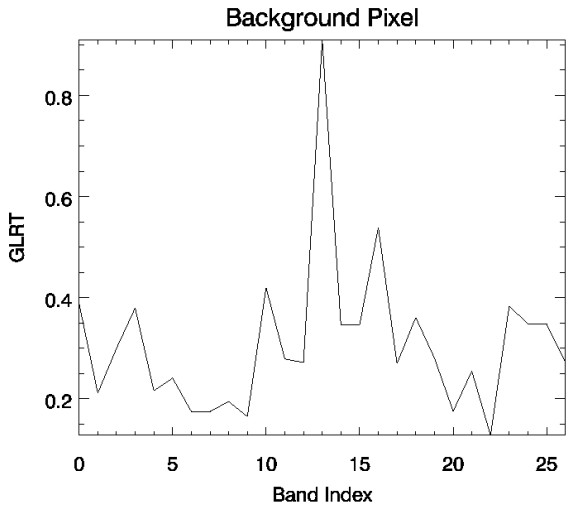

Figure 9. GLRT results for a background pixel. Note that the values are lower than Figures 5 and 7.

will be investigated using a multiple slab model instead of the single slab model. Also, multiple gas releases in a single plume will be investigated. Finally, a comparison will be made to the Thai and Healey (2002)[4] method which utilizes SVD as the means of obtaining basis vectors.

ACKNOWLEDGMENTS

The Office of Naval Research Multi-disciplinary University Research Initiative "Model-based Hyperspectral Exploitation Algorithm Development" no. N00014-01-1-0867 funded this project.

REFERENCES

1. K. Lee, *A subpixel scale target detection algorithm for hyperspectral imagery.* PhD thesis, Rochester Institute of Technology, 2003.
2. J. Schott, K. Lee, R. Raqueño, G. Hoffmann, and G. Healey, "A subpixel target detection technique based on the invariance approach," in *AVIRIS Airborne Geoscience workshop Proceedings*, February 2003.
3. J. Lisowski and C. Cook, "A svd method for spectral decomposition and classification of ares data," *SPIE* **2821**(15), pp. 14–19, 1996.
4. B. Thai and G. Healey, "Invariant subpixel material detection in hyperspectral imagery," *IEEE Trans. Geo. Rem. Sens.* **40**(3), pp. 599–608, 2002.
5. S. Young, "Detection and quantification of gases in industrial-stack plumes using thermal-infrared hyperspectral imaging," Tech. Rep. ATR-2002(8407)-1, Aerospace Corporation, 2002.
6. J. Schott, S. Brown, R. Raqueño, H. Gross, and G. Robinson, "An advanced synthetic image generation model and its application to multi/hyperspectral algorithm development," *Can. J. Rem. Sen.* **25**(2), pp. 99–111, 1999.
7. P. Bajorski, E. Ientillucci, and J. Schott, "Comparison of basis-vector selection methods for target and background subspaces as applied to subpixel target detection," in *Algorithms and Technologies for Multspectral, Hyperspectral, and Ultraspectral Imagery X, Proceeding of SPIE, v. 5425*, 2004.
8. S. Sharp *et al.*, "Creation of 0.10 cm^{-1} resolution, quantitative, infrared spectral libraries for gas samples," in *Vibrational Spectroscopy-Based Sensor Systems, Proceedings of SPIE, v. 4577*, S. Christesen and A.J. Sedlacek, III, eds., pp. 12–24, 2001.

9. E. Ientilucci and S. Brown, "Advances in wide area hyperspectral image simulation," in *Conference on Targets & Backgrounds IX: Characterization and Representation, Proceedings of SPIE, v. 5075*, pp. 110–121, 2003.
10. J. Halitsky, "A jet plume model for short stacks," *JAPCA Note-Book* **39**(6), pp. 856–858, 1989.
11. S. Kuo, J. Schott, and C. Chang, "Synthetic image generation of chemical plumes for hyperspectral applications," *Opt. Eng.* **39**(4), pp. 1047–1056, 2000.